

Location of the tricritical point for the melting of commensurate solid krypton on ZYX graphite

R. M. Suter and N. J. Colella

*Department of Physics and Center for the Joining of Materials, Carnegie-Mellon University,
Pittsburgh, Pennsylvania 15213*

R. Gangwar

*Department of Physics, Carnegie-Mellon University,
Pittsburgh, Pennsylvania 15213*

(Received 27 September 1984)

Detailed vapor-pressure isotherms of krypton on Union Carbide's ZYX exfoliated graphite are used to determine the distribution of absorption potentials and to locate the tricritical point where the melting of the commensurate krypton solid becomes continuous. We find from isotherms in the fluid-solid coexistence region an asymmetric, 1.5-K full width at half maximum distribution, comparable to other exfoliated graphites. A least-squares-fitting procedure indicates a tricritical point at 117 ± 2 K, in agreement with previous thermodynamic experiments but in sharp contrast to recent x-ray scattering experiments on the same type of substrate.

The nature of the melting transitions of commensurate adsorbed solids is a matter of theoretical¹⁻⁵ and experimental⁶⁻¹² controversy. The prototypical experimental systems are krypton and molecular nitrogen adsorbed on graphite, which both form $\sqrt{3} \times \sqrt{3} R 30^\circ$ commensurate solids. From among the variety of issues surrounding the nature of the phase diagrams of these systems, we focus attention on the position of the tricritical point where the melting transition becomes continuous. Until recently both systems were believed to have tricritical points at coverages close to one monolayer and at temperatures well below the maximum for solid formation.^{6,12} However, recent x-ray scattering data on krypton⁹ and thermodynamic measurements on N₂ (Ref. 11) are interpreted as indicating tricritical points at higher coverages and temperatures. In the present Rapid Communication, we use quantitative analysis of precise, low-noise vapor-pressure isotherms on Union Carbide's ZYX exfoliated graphite to argue that for krypton the tricritical point is located at 117 ± 2 K and below one monolayer coverage, as previously believed. Our analysis includes the first determination of the distribution function giving the fractional area of the sample per unit adsorption potential.

Our isotherm measurements are carried out with a unique automated apparatus. The construction of the system is to a large extent standard, using MKS Baritron pressure sensors and a Displex cryostat to cool the oxygen free high conductivity (OFHC) copper sample cell. However, as demonstrated in Fig. 1, the careful equilibration made possible by automation leads to low-noise isotherms from which the isothermal compressibility of the film can be reliably calculated over a three decade range. The low-noise level also makes possible the quantitative, least-squares-fitting analysis used below. We use a uniform and stringent criterion to determine pressure equilibration: the pressure must be constant to better than a part in 10^4 over a period of at least 10 min before equilibrium is said to have been achieved. Automation is particularly important for experiments on ZYX since we frequently have to wait as long as 2 h for equilibration. Details of the apparatus and procedure will be published separately.¹³

The isothermal compressibility shown in Fig. 1(b) is com-

puted from a finite difference approximation to the density derivative,

$$\kappa_T = \rho^{-2} (\partial \rho / \partial \mu)_T, \quad (1)$$

with ρ being the observed isotherm data divided by the sample area. The chemical potential of the film is deduced

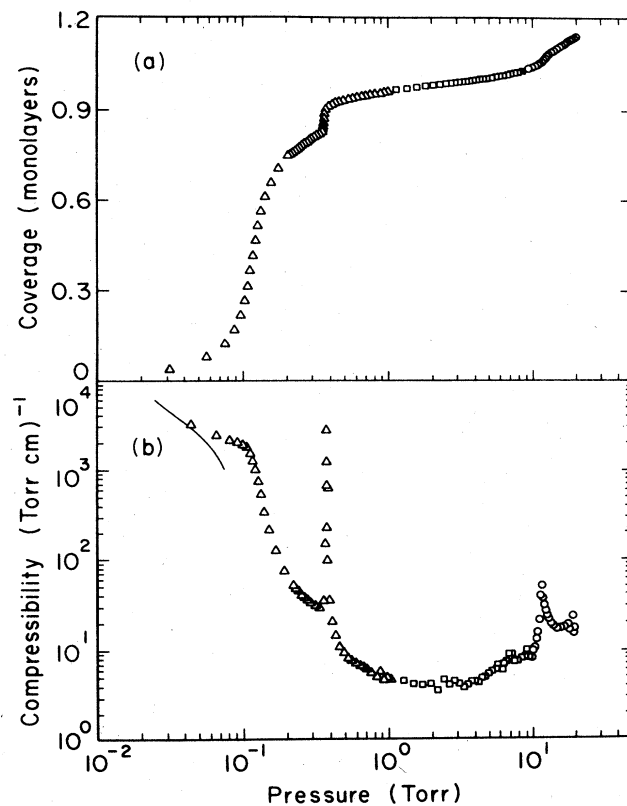


FIG. 1. (a) Isotherm and (b) compressibility of Kr on ZYX graphite at 100 K. The data are from three separate runs, each within 0.15 K of 100 K. The solid line in (b) gives the two-dimensional ideal-gas compressibility.

from that of the vapor, using the ideal-gas approximation. At low pressure and density, the compressibility is large, approaching that of an ideal two-dimensional gas at coverages less than 0.06 monolayer. Peaks in κ_T at 0.37 and 11.7 Torr correspond to transitions into the commensurate solid and domain-wall fluid phases, respectively.^{8,9}

Adsorption potential heterogeneity. The effects of finite size and heterogeneity of the adsorption potential on vapor-pressure isotherms have been discussed in Refs. 14 and 15. Both lead to a smearing of the ideal behavior. If, as we argue below, finite-size effects can be neglected, the degree of variation of the chemical potential across a coexistence region directly reflects the distribution of adsorption potentials. The observed isotherm is the convolution of an ideal isotherm with the adsorption potential distribution function¹⁵

$$O(\mu) = \int_{-\infty}^{+\infty} d\mu' g(\mu' - \mu) I(\mu') \quad (2)$$

where $O(\mu)$ is the observed isotherm as a function of chemical potential, $I(\mu)$ is the ideal system isotherm, and g is the distribution function giving the fraction of the sample area having an adsorption potential shifted by $\mu' - \mu$ relative to an arbitrary reference value. Equation (2) is identical to Eq. (3.2) of Ref. 15 with a change of integration variable.

According to (2), plots of $O(\mu)$ at different temperatures in a coexistence region should have a universal shape. Figure 2 shows that for our Kr on ZYX isotherms, this does indeed occur for data between 95 and 110 K, where the fluid-commensurate-solid transition is strongly first order. We have normalized the density discontinuities so that the coexistence region has $-1 < \rho < 1$. We take the success of the data collapsing in Fig. 2 to indicate that finite-size effects are not the primary determinants of the observed rounding. Using the convolution formula (2), we have fitted this composite reduced data to a piecewise linear ideal

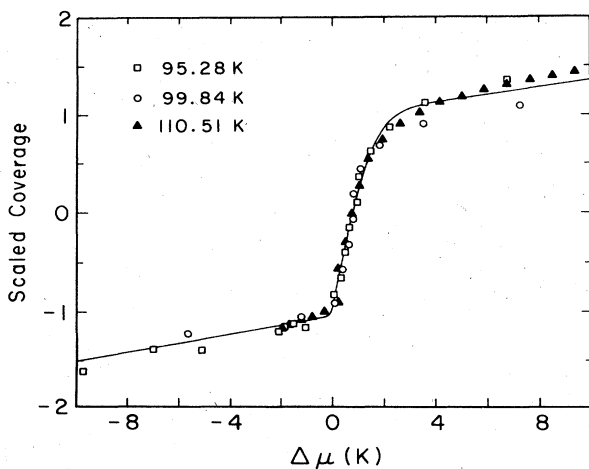


FIG. 2. Three reduced isotherms near the fluid-solid coexistence region. The data have been shifted horizontally and the density scales have been normalized so that the fitted ideal isotherm has a discontinuity of two. The actual size of the density discontinuity varies by a factor of 5 from 95 to 110 K. In the ~ 2 -K-wide transition region, the data have similar shapes while outside this region some variation of behavior in the uniform phases is observed. The solid line is the least-squares fit yielding the adsorption potential distribution function.

step convolved with an approximation for the distribution function. We have modeled g by a pair of half Gaussians

$$g(\Delta\mu) = 2[\sqrt{\pi}(\sigma_1 + \sigma_2)]^{-1} \times \begin{cases} \exp[-(\Delta\mu)^2/\sigma_1^2], & \Delta\mu \leq 0 \\ \exp[-(\Delta\mu)^2/\sigma_2^2], & \Delta\mu \geq 0 \end{cases} \quad (3)$$

This form is chosen due to the asymmetric shape of the isotherms. The low density of fluid side has a sharp break in slope which corresponds to a narrow distribution, whereas the high density or solid side is more rounded. The deduced Gaussian widths are $\sigma_1 = 0.07 \pm 0.05$ K and $\sigma_2 = 1.7 \pm 0.1$ K. The full width at half maximum is 1.5 K, which should be compared to the computed adsorption potential of 1430 K.¹⁶ This full width is less than or equal to widths observed on other forms of exfoliated graphite.^{10,11} Thus, ZYX appears to be an optimal exfoliated substrate for studies of phase transitions. It has a 2000 Å surface coherence length¹⁷ and the adsorption potential is uniform to 0.1%.

Data near the tricritical point. To locate the tricritical point for the melting of the krypton commensurate solid, we fit each isotherm with the piecewise linear ideal form convolved with the *fixed* distribution function determined above. A failure of this functional form to fit the data should signal a change in the nature of the transition. We neglect the fact that, in a weakly first-order region, the ideal isotherm will contain not only a jump but also precritical curvature corresponding to the growth of κ_T . This curvature grows into an inflection point as the first-order density jump goes to zero. Unfortunately, the smearing due to inhomogeneity makes this interesting precursor behavior extremely difficult to detect.

In Fig. 3, we show a series of isotherms along with the fits described above. It is clear that, as T is raised, the

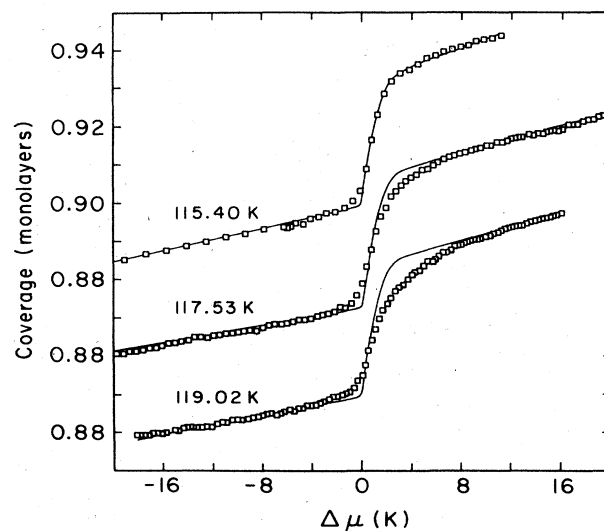


FIG. 3. Fits to isotherms using a piecewise linear ideal form and the distribution of adsorption potentials obtained from the data of Fig. 2. The failure of the fits at higher temperatures indicates a change in the character of the transition. For the 119.02-K data, the parameters describing the solid phase away from the transition were fixed in order to obtain the observed compressibility; otherwise, the least-squares routine chose an unphysically large solid compressibility in order to better fit the transition region.

rounding becomes more dramatic than that generated by the inhomogeneity distribution. This is precisely the behavior expected near a continuous transition. From Figs. 2 and 3, it can be seen that excellent fits are obtained using the piecewise linear ideal isotherm for data between 95 and 115.4 K. However, between 115.4 and 119.02 K, the χ^2 per degree of freedom increases by a factor of 7 and the quality of fit is seen to be visibly degraded. We conclude that there is a tricritical point at 117 ± 2 K, as expected on the basis of heat-capacity experiments on Grafoil⁶ and isotherm measurements on vermicular graphite.¹⁰ Thus, thermodynamic data on substrates with surface coherence lengths ranging from 100 to 2000 Å indicate that the krypton commensurate solid melts continuously over the entire high-temperature region of the phase diagram. As discussed below, this contrasts sharply with recent x-ray scattering evidence.⁹

While the above analysis appears to establish the presence of the tricritical point at 117 K, it is interesting to ask whether the same distribution of adsorption potentials can fit data in the continuous region. We obtain an ideal form for the isotherm near a continuous transition by assuming a power-law divergence of the compressibility,

$$\kappa_T = \begin{cases} K_0(\mu_t - \mu)^{-w} + K_<, & \mu < \mu_c, \\ rK_0(\mu - \mu_t)^{-w'} + K_>, & \mu > \mu_c. \end{cases} \quad (4)$$

$K_<$ and $K_>$ are compressibilities characterizing the low- and high-density phases, respectively, r is the power-law amplitude ratio, and K_0 is the critical amplitude in the fluid phase. w and w' are effective critical exponents and we assume $w = w'$. Separating variables in (1) and integrating yields the ideal form

$$\rho(\mu) = \left(\rho_0^{-1} + \int_{\mu_0}^{\mu} d\mu \kappa_T \right)^{-1}. \quad (5)$$

ρ_0 is the density at a reference chemical potential, μ_0 . This form, with (4), is used in (2). Figure 4 illustrates that fits which reproduce the data to better than 10^{-3} of a monolayer are obtained from the power-law formula, keeping the adsorption potential distribution fixed to that obtained at low temperatures. This is convincing evidence that the

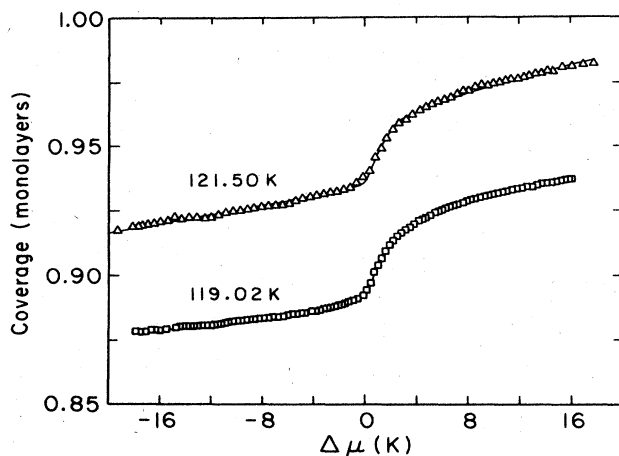


FIG. 4. Fits to isotherms using an ideal form appropriate for a continuous transition (see text). The deviations of the fit from the data points at 119 K are smaller than the size of the symbols. The increased noise in the data at 121.5 K is due to the higher pressure at which the transition takes place.

transition above 117 K is continuous with a power-law divergence in the compressibility. At lower temperatures, the power-law fits become progressively worse; at and below 100 K, good fits were not obtained.

The smearing of the continuous transitions severely limits interpretation of the data. It is evident that a continuous transition is observed and, from x-ray scattering experiments,⁹ it can be assumed that finite-size effects are small. However, adjustment of the distribution function widths yields significant changes in the exponent w obtained from the fits and the widths cannot be assumed to be the same as those seen in the first-order region. Macroscopic inhomogeneities (for example, variations from crystallite to crystallite) would generate a distribution similar to that seen in the first-order region whereas local, microscopic variations, which can be modeled as a random field, could yield a sharp transition.¹⁸ The ZYX sample may be a combination of these extremes and therefore require an intermediate distribution of critical chemical potentials.

Discussion. It is clear that accurate vapor-pressure isotherms can yield quantitative information about the behavior of phase transitions in adsorbed films. The adsorption potential distribution obtained here should find application in other experiments on ZYX graphite. However, the present work demonstrates that, at least near continuous transitions, smearing due to inhomogeneity in the adsorption potential severely limits interpretation. The experiment is limited by the sample rather than by technique.

The absence of critical scattering in x-ray experiments⁹ crossing the low-density fluid to commensurate solid phase boundary is puzzling. Our measurements agree quantitatively with the *position* of the phase boundaries reported in Ref. 9 between 115 and 125 K (see their Fig. 1), but while we see a continuous transition between 117 and 121 K (our data at 125 K being insufficiently precise for quantitative analysis), Specht *et al.*⁹ interpret their data at and above 124 K as indicating a first-order transition. We cannot rule out a small first-order jump in our isotherms, but the power-law behavior we see would lead us to expect a significant growth of correlations before the transition. We can only note here that (i) the temperature ranges just described are nonoverlapping, (ii) the pressure region over which the continuous transition takes place is narrow ($\sim 3\%$ of the transition pressure), and (iii) the coverage trajectories of the constant pressure scans in the x-ray experiment are unknown. In future work, we will use a small volume gas-handling system to take isotherm data up to 130 K; we will check the nature of the transitions and determine the coverage path of the x-ray scans.

A recent vapor-pressure isotherm experiment using a graphite foam substrate has placed the tricritical point for melting of the N_2 commensurate solid at 85.4 K and 1.2 monolayers coverage.¹¹ As pointed out by Specht *et al.*⁹ this result is consistent with the x-ray scattering results for Kr. However, we prefer to interpret the data of Miner, Chan, and Migone¹¹ as indicating a tricritical point between 82 and 84 K and near one monolayer coverage, as concluded earlier by Larher.¹² Between 82 and 84 K, we see the same qualitative change in the shape of the N_2 isotherms as we see in our Kr data at 117 K. In addition, the data of Miner *et al.*¹¹ above 85.4 K do not appear to contain any phase transition since there is no indication of a step or an inflection point corresponding to a divergent compressibility [see Eq. (5) and Fig. 4]. The high-temperature data appear to indicate a

rapidly decreasing compressibility as might be expected on passing from a low- to a high-density fluid above the maximum temperature for solid formation. Reassignment of the tricritical temperature to the value given by Larher would place the N_2 point in a position somewhat closer to that found here for Kr.

We would like to thank R. B. Griffiths, K. Niskanen, P. M. Horn, and P. Dimon for helpful discussions and encouragement. This work was supported in part by a grant from the Samuel and Emma Winter Foundation and by the National Science Foundation through Materials Research Laboratory Grant No. DMR8119507.

-
- ¹A. N. Berker, S. Ostlund, and F. A. Putnam, *Phys. Rev. B* **17**, 3650 (1978).
²S. Ostlund and A. N. Berker, *Phys. Rev. Lett.* **42**, 843 (1979).
³D. A. Huse and M. E. Fisher, *Phys. Rev. Lett.* **49**, 793 (1982).
⁴D. A. Huse and M. E. Fisher, *Phys. Rev. B* **29**, 239 (1984).
⁵D. A. Huse, *Phys. Rev. B* **29**, 5031 (1984).
⁶D. M. Butler, J. A. Litzinger, G. A. Stewart, and R. B. Griffiths, *Phys. Rev. Lett.* **42**, 1289 (1979).
⁷D. M. Butler, J. A. Litzinger, and G. A. Stewart, *Phys. Rev. Lett.* **44**, 466 (1980).
⁸P. W. Stephens, P. A. Heiney, R. J. Birgeneau, P. M. Horn, D. E. Moncton, and G. S. Brown, *Phys. Rev. B* **29**, 3512 (1984).
⁹E. D. Specht, M. Sutton, R. J. Birgeneau, D. E. Moncton, and P. M. Horn, *Phys. Rev. B* **30**, 1589 (1984).
¹⁰Y. Larher and A. Terlain, *J. Chem. Phys.* **72**, 1052 (1980).
¹¹K. D. Miner, Jr., M. H. W. Chan, and A. D. Migone, *Phys. Rev. Lett.* **51**, 1465 (1983).
¹²Y. Larher, *J. Chem. Phys.* **68**, 2257 (1978).
¹³N. J. Colella, R. Gangwar, and R. M. Suter (unpublished).
¹⁴J. G. Dash and R. D. Puff, *Phys. Rev. B* **24**, 295 (1981).
¹⁵R. E. Ecke, J. G. Dash, and R. D. Puff, *Phys. Rev. B* **26**, 1288 (1982).
¹⁶G. Vidali and M. W. Cole, *Phys. Rev. B* **29**, 6736 (1984).
¹⁷R. J. Birgeneau, P. A. Heiney, and J. P. Pelz, *Physica* **109&110B**, 1785 (1982).
¹⁸G. Grinstein and S-k. Ma, *Phys. Rev. B* **28**, 2588 (1983), and references therein.